Mustafa U. Demirci and Clark T.-C. Nguyen, "A Low Impedance VHF Micromechanical Filter Using Coupled-Array Composite Resonators," *Dig. Of Tech. papers*, the 13th Int. Conf. on Solid-State Sensors & Actuators (Transducers'05), Seoul, Korea, June 5-9, 2005, pp. 2131-2134.

A LOW IMPEDANCE VHF MICROMECHANICAL FILTER USING COUPLED-ARRAY COMPOSITE RESONATORS

Mustafa U. Demirci and Clark T.-C. Nguyen

Center for Wireless Integrated Micro Systems
Department of Electrical Engineering and Computer Science
University of Michigan, Ann Arbor, Michigan 48109-2122, USA

ABSTRACT

By using mechanically-coupled flexural-mode square resonator arrays as "composite" resonators, the impedance of a 68.1-MHz (VHF), capacitively-transduced micromechanical filter has been lowered to point of allowing *L*-network-aided matching to 50Ω termination impedances, while also exhibiting less than 2.7dB insertion loss (*IL*) for a 190kHz passband width (0.28% bandwidth). The use of composite arrays to replace previous single resonators in a series filter topology not only allows a reduction in filter termination resistance by a factor ideally equal to the number of resonators in the array, but also a reduction in filter bandwidth by this same factor—an important feature for channel-select applications. Although array *Q* values are smaller than the *Q* of a stand-alone square resonator, they are still sufficient for excellent filter performance.

Keywords: array, bandpass filter, impedance, quality factor, RF MEMS.

1. INTRODUCTION

The increasing demand for wireless devices that support a multitude of communication modes (e.g., voice, video, data, etc.), all in one small handset, has spurred great interest in technologies capable of miniaturizing the multi-band reconfigurable RF front-ends that enable such multi-function capability. Recently, vibrating micromechanical resonator technology, with its ability to realize highly selective, low-loss, on-chip filters [1]-[4] suitable for band- or even channel-selecting filter banks [5], has emerged as an attractive approach towards miniaturized multi-band wireless reconfigurability. To date, VHF micromechanical filters [2][3] and mixer-filters [6] have been demonstrated with impressive frequency characteristics and insertion losses; however the impedances of these filters have so far not been small enough to allow discrete matching to conventional antenna impedances.

In part to address the impedance issue, this paper presents a new filter architecture that uses mechanically coupled arrays of *N*-resonators [7] instead of single resonators, to provide (1) *N*-times reduction in the termination resistance of the filter, and (2) nearly *N*-times larger coupler attachment stiffness than that of a single resonator, which in turn allows a bandwidth approximately *N*-times smaller than that of previous micromechanical filters [1]-[3]. Using this architecture with 11-resonator arrays (c.f. Fig. 1), a VHF filter has been demonstrated with an insertion of loss less than 2.7dB, which is the lowest measured to date for any *micromechanical* filter in the popular 70MHz super-heterodyne wireless IF range. This is also the first time the impedance of a multi-pole capacitively-

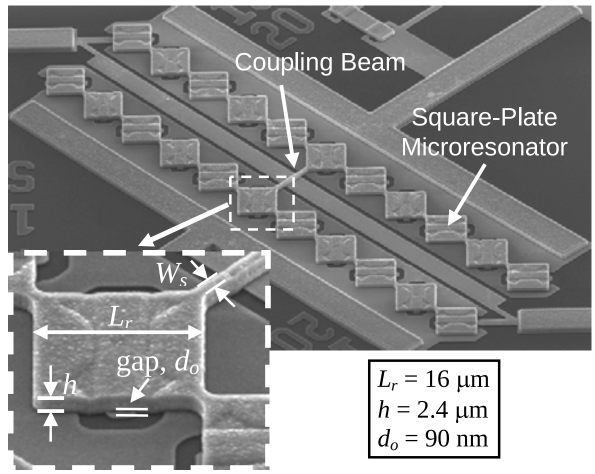

Fig. 1: SEM of a fabricated coupled-resonator array filter utilizing arrays of eleven square microresonators.

transduced filter has been low enough to allow *L*-network-aided matching to 50Ω. Furthermore, advantage (2) eliminates the need for sub-μm coupling beam dimensions that would otherwise be needed to achieve the 200kHz IF filter bandwidth required by GSM wireless handsets. This greatly relaxes fabrication tolerances, thereby greatly enhancing control of the filter bandwidth. This work extends the concept of integrated micromechanical circuit technology [5] to medium-scale integration (MSI) levels, using up to 43 resonators and links.

2. DEVICE STRUCTURE AND OPERATION

Fig. 2 presents a schematic of the coupled-resonator array filter concept, comprised of two square-plate microresonator arrays [7] connected by a torsional coupling beam. Each array consists of *N* transverse-mode square plate microresonators suspended 90 nm above capacitive-transducer electrodes by center stems. The square plates are mechanically coupled at their corners via identical short stiff stubs that force all resonators to vibrate at the same frequency in unison when properly excited. While the array sustains multiple resonance modes, the electrodes underneath are placed to accentuate one mode of the coupled array while suppressing others. This is done by imposing properly phased AC forces on constituent resonators that emphasize phasings associated with the desired mode of the array while counteracting all others [7]. The electrodes of the resonators are electrically connected to each other for excitation with a common AC voltage and the currents from each resonator add to generate an *N* times larger output. In effect, via mechanical coupling, each resonator array behaves like a single com-

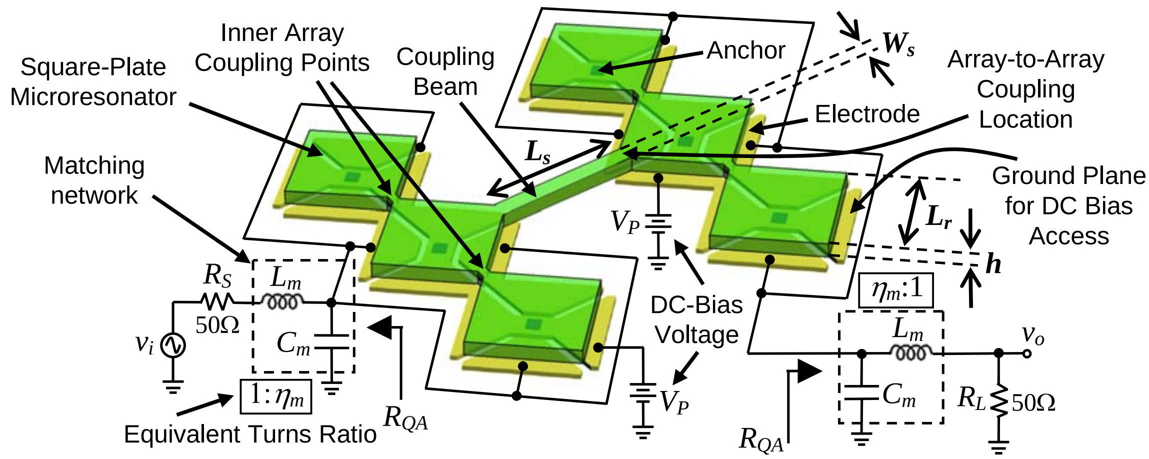

Fig. 2: Perspective view of a coupled-resonator array filter utilizing three-resonator arrays (i.e., N=3).

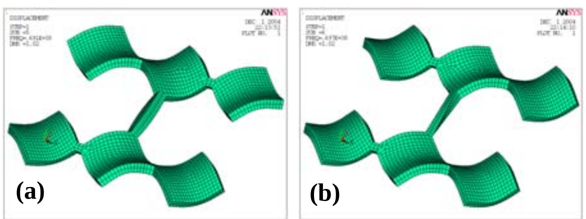

*Fig. 3: ANSYS-simulated **(a)** in-phase and **(b)** out-of-phase mode shapes of the coupled-array filter of Fig. 2.*

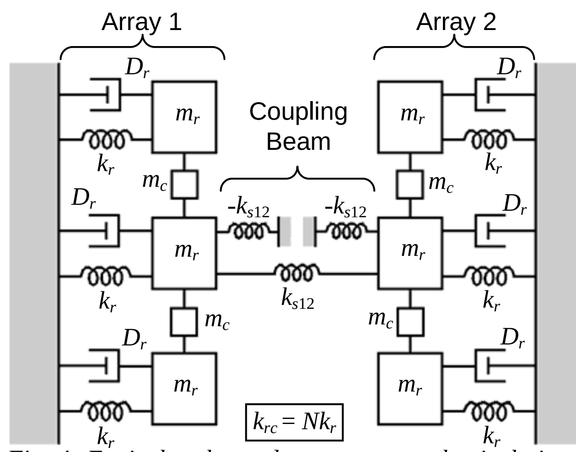

Fig. 4: Equivalent lumped parameter mechanical circuit of the coupled-resonator array of Fig. 2.

posite resonator with an N times lower impedance. In this way, the overall filter structure condenses to a coupled two-resonator series filter topology [2], with two modes of vibration, depicted in Fig. 3, as simulated by ANSYS.

The excitation electrodes of the first array (on the left) form the input electrode of the filter and the electrodes of the second array form the output electrode. To operate the device, a DC bias is applied to the filter structure via the ground plane underneath, which connects the anchors of each resonator. The input AC signal v_i with 50Ω source resistance is applied to the input electrode through an L-matching network. When the frequency of v_i falls within the filter passband, the mechanical structure vibrates with an overall mode shape that combines those of Fig. 3. This creates a motional output current, which then passes through another L-network and generates a voltage on the 50Ω load impedance. The matching networks transform the 50Ω source and load to provide the required impedance for proper filter termination [1][2].

3. ARRAY FILTER DESIGN

The flexural square-plate microresonators comprising the coupled arrays are designed to have identical dimensions, each with resonance frequency given by [8]

$$f_{or} = 0.9697\sqrt{\frac{E}{\rho}}\frac{h}{L_r^2} \qquad (1)$$

where h is the structure thickness; L_r is the plate side length shown in Fig. 2; and E, ρ, and ν are the Young's modulus, density, and Poisson ratio, respectively, of its structural material. Since the short coupling stubs add negligible mass and ideally no stiffness (since they are at nodal locations) to the arrays in the selected mode, the resonance frequency of the arrays deviate only very slightly from (1). By designing the arrays to be identical, then coupling them using a torsional quarter-wavelength beam, the filter passband will be centered around the common array resonance frequency.

Filter Coupling Beam.

For a two-pole mechanical filter with center frequency f_o, the required coupling beam spring constant k_{s12} to achieve a desired bandwidth BW is given by [2]

$$k_{s12} = k_{rc}\left(\frac{BW}{f_o}\right)k_{12} \qquad (2)$$

where k_{12} is the normalized coupling coefficient between resonator tanks for a given filter type (i.e., Butterworth, Chebyshev, etc.) [9], and k_{rc} is the effective spring constant of the "composite" resonator at the array-to-array coupling location, which can be determined by analysis of the equivalent lumped parameter mechanical circuit of the coupled array presented in Fig. 4. Here, each square resonator is represented by a mass, spring, damper system corresponding to the location where the single resonator of the composite array is attached to the array-to-array coupling beam; the array-to-array coupling beam com-

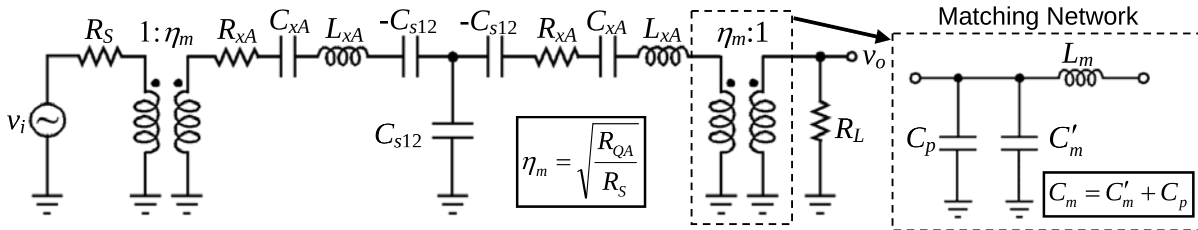

Fig. 6: Electrical LCR equivalent circuit of the coupled-resonator array filter of Fig. 2.

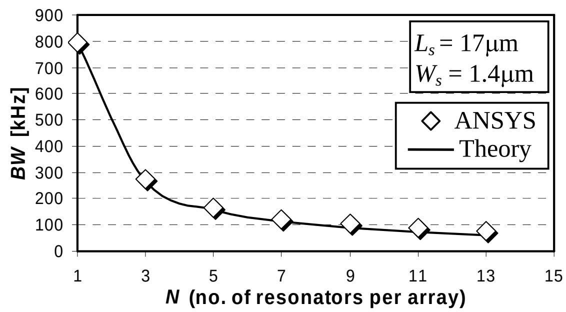

Fig. 5: ANSYS-simulated and analytically-calculated bandwidth (BW) versus N (number of resonators per array) plots for the coupled-array filter of Fig. 2.

prises a network of positive and negative spings [1]; and the m_c's represent the short coupling stubs of the array. The stiffnesses of the N constituent resonators of the array are in parallel, so add to yield a total array composite spring constant at the array-to-array coupling location given by

$$k_{rc} = Nk_r \tag{3}$$

where k_r is the stiffness of a single square plate resonator. Using (3) in (2), the coupling beam spring constant needed to affect a bandwidth BW becomes

$$k_{s12} = Nk_r\left(\frac{BW}{f_o}\right)k_{12}, \tag{4}$$

which shows that an array with N resonators requires an N times larger coupling beam stiffness than needed by a stand-alone resonator to achieve a given bandwidth. (This is a good thing.) Also, for a given k_{s12}, the bandwidth can be reduced simply by increasing N (by coupling more resonators into the array).

Fig. 5 presents plots of bandwidth BW versus N for the coupled-array filter of Fig. 2 obtained by (4) (the curve) and as simulated in ANSYS (the points). Here, both methods are in agreement and predict that the bandwidth decreases with increasing N. This is a very convenient utility for filter design, especially for resonator types for which low velocity coupling is not straightforward, such as the square-plate resonators of this work. For such resonators, implementing a small percent bandwidth filter with no low-velocity coupling often necessitates submicron coupling beam dimensions. In particular, without arraying, a square resonator filter would require coupling beam widths on the order of 0.25 μm to achieve the 200 kHz IF bandwidth specification of GSM wireless handsets. On the other hand, the use of array composite resonators allows much larger coupler widths, on the order of 1.6 μm, to achieve the same bandwidth. This greatly relaxes fabrication tolerances and enhances control of the filter bandwidth.

Equivalent circuit.

Fig. 6 presents the electrical equivalent circuit of the filter where *LCR* tanks model the arrays, and a capacitive *T*-network represents the torsional quarter-wavelength coupling beam. The element values in the *LCR*'s are determined by the mass, spring stiffness, and damping, at the coupling location of each array, and can be expressed as

$$R_{xA} = \frac{\sqrt{k_r m_r}}{NQ_A\eta_x^2}, L_{xA} = \frac{m_r}{N\eta_x^2}, C_{xA} = \frac{N\eta_x^2}{k_r}, \eta_x = V_P\frac{\partial C}{\partial x} \tag{5}$$

where η_x, $\partial C/\partial x$, and m_r, are the electromechanical coupling coefficient, change in the resonator-to-electrode capacitance per unit displacement, and mass, of a single square-plate resonator, respectively; V_P is the DC bias; and Q_A is the quality factor of the array. The transformers in the equivalent circuit model the impedance matching *L*-networks.

Filter Termination.

To flatten the filter passband and achieve the designed amount of ripple, the Q's of the end resonators must be controlled (i.e., loaded) via resistive termination at the input and output electrodes. The value of the impedance required to terminate a coupled array filter is given by

$$R_{QA} = \left(\frac{Q_A}{q_i Q_{fltr}} - 1\right)R_{xA} \cong \frac{\sqrt{k_r m_r}}{Nq_i Q_{fltr}\eta_x^2} \cong \frac{R_Q}{N} \tag{6}$$

where the approximation is valid for $Q_A >> q_i Q_{fltr}$; Q_A and Q_{fltr} are the array and filter quality factors, respectively; R_Q is the impedance required to terminate a filter that uses stand-alone end resonators instead of arrays; and q_i is a normalized Q parameter obtained from a filter cookbook [9]. From (6), the use of N-resonator arrays instead of single resonators provides an N times reduction in the filter termination impedance, as long as Q_A is sufficiently larger than $q_i Q_{fltr}$.

The *L*-matching networks [10] at the input and output electrodes of the filter transform the 50Ω source and load impedances (i.e., R_S and R_L) to the filter termination impedance R_{QA}. Shunt parasitic capacitors at the input and output of the filter (i.e., C_p in Fig. 6) are also conveniently incorporated into the matching network capacitors C_m as seen in Fig. 6.

The insertion loss of the filter is given by

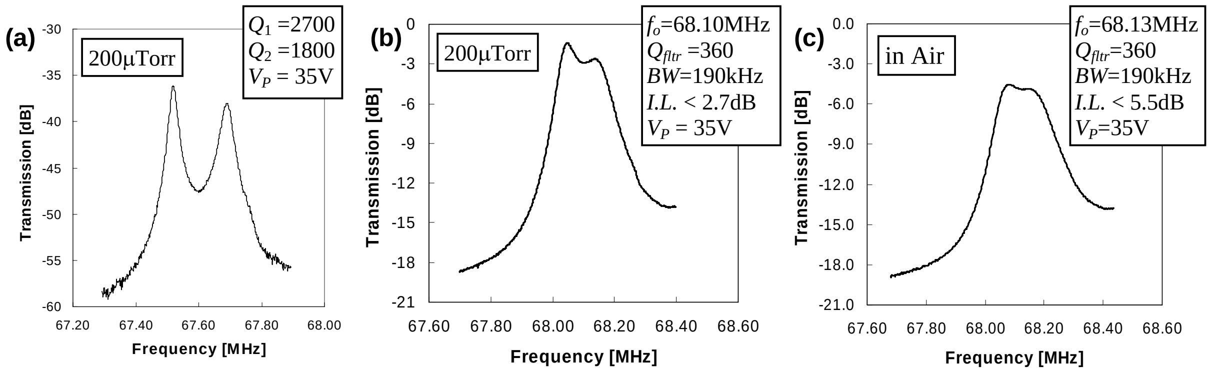

Fig. 7: Measured frequency characteristics for the coupled-resonator array filter of Fig. 1 ***(a)*** *without impedance matching (unterminated resonance characteristics);* ***(b)*** *using the configuration of Fig. 2; and* ***(c)*** *under atmospheric pressure using the same hook-up.*

Table I: Array Filter Design and Performance

Parameter	Value	Parameter	Value
f_o	68.10 MHz	V_P	35 V
BW	190 kHz	L_s	17 μm
Q_{fltr}	360	W_s	1.4 μm
L_r	16.0 μm	L_m	1.8 μH
h	2.4 μm	C_m	3.0 pF
d_o	90 nm	η_m	15.5
Q	12,000	Q_A	1,800
R_x	6.6 kΩ	R_{xA}	4 kΩ
R_Q	170 kΩ*	R_{QA}	12 kΩ**

Variable definitions are given throughout the text.
* Calculated using Q and R_x.
** Calculated using Q_A and R_{xA}.

$$IL = 20\log\left(\frac{R_{QA}+R_{xA}}{R_{QA}}\right) = 20\log\left(\frac{Q_A}{Q_A - q_i Q_{fltr}}\right). \quad (7)$$

4. EXPERIMENTAL RESULTS

Coupled-resonator array filters were designed to the specifications of Table I using the theory of Section 3 and fabricated via a now "conventional" thin-vertical-gap surface micromachining process [2]. Fig. 1 presents the SEM of a micromechanical filter utilizing 11-resonator array composite resonators.

Fig. 7(a) presents the frequency characteristics of the coupled-resonator array filter of Fig. 1 measured under 200μTorr vacuum without impedance matching in order to isolate the two modes of Fig. 3. As shown, the peaks have slightly different Q's of 2,700 and 1,800, possibly due to differences in anchor losses in the two modes [3]. Furthermore, the array Q values Q_A are smaller than the Q of 12,000 exhibited by a stand-alone square resonator on the same die, and this decreases the R_x reduction factor to a value less than N=11. Despite this, as seen in Table I, the filter actually still attains a 14x reduction in R_Q, which is larger than the expected 11x. This occurs because the Q_A of the array is 6.7x smaller than that of a single resonator, which from the leftmost form of (6), actually contributes to a decrease in R_{QA}, at the cost of an increase in insertion loss.

Fig. 7(b) presents the frequency spectrum of the 68.1-MHz filter of Fig. 1 measured under 200μTorr vacuum using the hook-up of Fig. 2, showing a bandwidth of 190kHz and an excellent insertion loss (IL) less than 2.7dB. This is not only the lowest insertion loss measured to date for any *micromechanical* filter in the popular 70MHz super-heterodyne wireless IF range, but is also the first time the impedance of such a capacitively-transduced filter has been low enough to allow matching to 50Ω. The "peaking" in the passband caused by differences in the Q's of the two modes of Fig. 3 actually achieves an IL of 1.5 dB.

Fig. 7 presents the spectrum for the same filter measured under atmospheric pressure, which shows a higher (but still acceptable) IL of ~5.5dB due to an air-damped decrease in the array Q's to 1,300 and 1,100, and almost no peaking, since viscous gas damping brings the Q's of the two modes down to almost the same value.

5. CONCLUSION

A two-pole 68.1-MHz micromechanical filter utilizing mechanically-coupled 11-resonator arrays as composite resonators has been demonstrated with termination impedances 14 times smaller than that of a filter implemented with single (non-arrayed) constituent resonators. The use of arraying not reduces impedances to the point of allowing matching to 50Ω via L-networks, but in raising the coupling beam stiffness needed to realize a given bandwidth, also permits the use of larger coupling beam dimensions for a given filter response. In doing so, arraying greatly improves the manufacturability of filters using MEMS technology and further encourages the use of vibrating RF MEMS in multi-band reconfigurable wireless applications.

REFERENCES

[1] K. Wang, *et al.*, *JMEMS*, 8(4), pp. 534-557, 1999.
[2] F. D. Bannon III, *et al.*, *JSSC*, vol. 35, no. 4, pp.512-526.
[3] A.-C. Wong, *et al.*, *Transducers'99*, pp. 1390-1393.
[4] S. Pourkamali, *et al.*, *MEMS'03*, pp. 702-705.
[5] C. T.-C. Nguyen, *CICC'04*, pp. 257-264.
[6] A.-C. Wong, *et al.*, *JMEMS*, 13(1), pp. 100-112, 2004.
[7] M. U. Demirci, *et al.*, *Transducers'03*, pp. 955-958.
[8] S. Timoshenko, *Vibration Problems in Engineering*, 1974.
[9] A. I. Zverev, *Handbook of Filter Synthesis*, 1967.
[10] D. M. Pozar, *Microwave Engineering*, 2005.